



Published in final edited form as:

Mol Neurobiol. 2018 May ; 55(5): 4403–4416. doi:10.1007/s12035-017-0653-9.

CRMP2 phosphorylation drives glioblastoma cell proliferation

Aubin Moutal¹, Lex Salas Villa¹, Seul Ki Yeon², Kyle T. Householder^{3,4}, Ki Duk Park², Rachael W. Sirianni^{3,4}, and Rajesh Khanna^{1,5,6,*}

¹Department of Pharmacology, College of Medicine, University of Arizona, Tucson, AZ, USA

²Center for Neuro-Medicine, Brain Science Institute, Korea Institute of Science and Technology, Seoul, 136-791, Republic of Korea

³Barrow Brain Tumor Research Center, Barrow Neurological Institute, 350 W. Thomas Rd., Phoenix, AZ 85013, USA

⁴School of Biological and Health Systems Engineering, Ira A. Fulton Schools of Engineering, Arizona State University, P.O. Box 879709, Tempe, AZ 85287, USA

⁵Department of Anesthesiology, College of Medicine, University of Arizona, Tucson, AZ, USA

⁶Neuroscience Graduate Interdisciplinary Program, College of Medicine, University of Arizona, Tucson, AZ, USA

Abstract

Glioblastoma (GBM) is an aggressive primary brain tumor. The rapid growth and the privileged provenance of the tumor within the brain contribute to its aggressivity and poor therapeutic targeting. A poor prognostic factor in glioblastoma is the deletion or mutation of the *Nf1* gene. This gene codes for the protein neurofibromin, a tumor suppressor gene that is known to interact with the collapsin response mediator protein 2 (CRMP2). CRMP2 expression and elevated expression of nuclear phosphorylated CRMP2 has recently been implicated in cancer progression. The CRMP2-neurofibromin interaction protects CRMP2 from its phosphorylation by cyclin dependent kinase 5 (Cdk5), an event linked to cancer progression. In three human glioblastoma cell lines (GL15, A172, and U87), we observed an inverse correlation between neurofibromin expression and CRMP2 phosphorylation levels. Glioblastoma cell proliferation was dependent on CRMP2 expression and phosphorylation by Cdk5 and glycogen synthase kinase 3 beta (GSK3 β). The CRMP2 phosphorylation inhibitor (*S*)-lacosamide reduces, in a concentration-dependent manner, glioblastoma cell proliferation and induced apoptosis in all three GBM cell lines tested. Since (*S*)-lacosamide is bioavailable in the brain, we tested its utility in an in vivo orthotopic model of GBM using GL261-LucNeo glioma cells. (*S*)-lacosamide decreased tumor size, as measured via in vivo bioluminescence imaging, by ~54% compared to vehicle control. Our results introduce CRMP2 expression and phosphorylation as a novel player in GBM proliferation and survival, which is enhanced by loss of *Nf1*.

*Corresponding Author: Dr. Rajesh Khanna, Department of Pharmacology, College of Medicine, University of Arizona, 1501 North Campbell Drive, P.O. Box 245050, Tucson, AZ 85724, USA; rkhanha@email.arizona.edu.

Conflict of Interest

The authors declare that they have no conflict of interest.

Keywords

CRMP2; phosphorylation; neurofibromin; glioblastoma; proliferation; (*S*)-Lacosamide

Introduction

Among central nervous system tumors, glioblastoma multiforme (GBM), a WHO grade IV astrocytoma, is the most aggressive form. Despite recent advances in treatment protocols [1] and advanced molecular studies [2,3], the median survival for GBM patients remains approximately 14 months [2]. Poor patient survival is due to a multitude of factors, including late stage at diagnosis, treatment resistance, and a lack of drugs capable of reaching invasive cells that reside behind the blood-brain barrier [2,4]. An important molecular signature in glioblastoma is the loss or mutation of the *Nf1* gene, which codes for the protein neurofibromin. *Nf1* alterations are negatively linked to GBM patients' survival [5–7] and are enriched in the mesenchymal subgroup of GBM [3]. Recurrence of GBM after treatment involves a shift towards a mesenchymal subtype [8,9]. Also, it was suggested that *Nf1* loss in GBM can happen over time even if the primary tumor did not initially show alteration of the *Nf1* gene [10]. Thus, *nf1* loss contributes to GBM recurrence and is linked to lower survival of patients. Neurofibromin is an anti-oncogene whose most established function is to inactivate the pro-oncogene Ras [11], an event that promotes gliomagenesis [12,13]. However, neurofibromin has other known protein partners that may facilitate pro-oncogenic mechanisms – one of these proteins is collapsin response mediator protein 2 (CRMP2).

CRMP2 is an axonal growth and guidance protein [14–16] that binds to the C-terminus of neurofibromin [17]. This protein-protein interaction inhibits CRMP2 phosphorylation by cyclin dependent kinase 5 (Cdk5), which in turn promotes neurite outgrowth [17]. Loss of neurofibromin results in increased CRMP2 phosphorylation by Cdk5 [17], an event linked to cancer progression [18,19]. Gain of CRMP2 phosphorylation at the Ser522 site by Cdk5 has been previously described in lymphoma [18], as well as in breast [18,20] and lung [12,21], cancers. Recently, loss of CRMP1 [22] and gain of CRMP5 [23] – two other members of the CRMP family – were reported to participate in glioblastoma oncogenic mechanisms. Since *nf1* loss is a hallmark in glioblastoma [5,6,3] and is linked to lower survival [5,6] and recurrence [8,9]; and neurofibromin inhibits CRMP2 phosphorylation by Cdk5 [17], an event linked to cancer progression [18,19], we hypothesized the CRMP2 phosphorylation is an important molecular event driving glioblastoma cell proliferation and survival.

Here we demonstrate that neurofibromin protein levels are inversely correlated with CRMP2 phosphorylation levels. Equally importantly, we demonstrate that CRMP2 expression promotes GBM cell proliferation. This novel function is governed by CRMP2's phosphorylation status since expressing phosphorylation-deficient CRMP2 mutants prevented CRMP2-dependent GBM cell proliferation. (*S*)-Lacosamide ((*S*)-LCM), an inactive analog of the clinically-approved small molecule anti-epileptic drug (*R*)-Lacosamide (Vimpat®)[24], inhibited CRMP2 phosphorylation at S522 [25–27] in three human GBM cell lines. (*S*)-lacosamide decreased in cell proliferation *in vitro*, which was linked to induction of apoptosis. In the final series of experiments, we evaluated the ability

of (S)-Lacosamide to inhibit growth of orthotopic tumors *in vivo*, in a syngeneic model of murine GBM.

Methods

Materials

Human cell lines GL15 [28], A172 (American Type Culture Collection [ATCC], Manassas, VA, USA; CRL_1620), U87 (ATCC® HTB-14™) were authenticated as reported previously [23] using Short Tandem Repeat DNA profiling and maintained in appropriate media. GL261-LucNeo glioma line was described earlier [29]. Antibodies used in this study are: anti-CRMP2 polyclonal antibody (Cat#2993, Sigma, St. Louis, MO); anti-neurofibromin N-terminal (Cat# sc-68, Santa Cruz biotechnology, Dallas, TX); CRMP2 pSer522 (Cat# CP2191, ECM Biosciences); and Actin (Cat# A2066, Sigma). For RNA interference, siRNA CRMP2 (5'-GTAAACTCCTTCCTCGTGT-3') (specificity validated previously [30,31]), and siRNA Control (Cat# 12935300) were obtained from Thermo Fisher Scientific (Waltham, MA). A BLAST search of siRNA sequences against the human transcriptome did not reveal potential off target effects. (S)-lacosamide ((S)-LCM) was synthesized as described previously [32]. Plasmids coding for *Discosoma sp.* red fluorescent protein (dsRed) fused to wildtype and phospho-deficient CRMP2 were as reported earlier by Dustrude and colleagues [31].

Nucleic acid transfection

Indicated cell lines were plated to reach 50% confluency on the next day. Transfection was done using Lipofectamine 2000 according to manufacturer's instructions. For siRNA transfections, a final concentration of 200nM was used. For plasmid transfection, a 2:1 Lipofectamine 2000:DNA ratio was used. In all cases, transfection was prepared in OptiMEM and added dropwise onto the cells. The media was changed 24h later and the cells used the next day (i.e., a total of 48h after transfection). Plasmid transfection was verified by dsRed fluorescence and knockdown was verified by Western blot.

Immunocytofluorescence

Indicated cells were grown on sterile glass coverslip ø15mm in 12 well plates. After 2 days in culture, cells were washed twice with phosphate buffered saline (PBS) and fixed using ice-cold methanol for 5 min. After removal, cells were allowed to dry at room temperature and conserved in PBS at 4°C until staining. Non-specific antibody binding sites were saturated with 3% [mass/vol] (bovine serum albumin (BSA) in PBS for 1h at room temperature, and then the indicated primary antibodies were incubated for 1h at room temperature in 3% BSA in PBS. Cells were washed 3 times for 5 min at room temperature with PBS, 3% BSA and secondary antibodies were added at 1/2000 dilution in PBS containing 3% BSA for 1h incubation at room temperature. After 3 washing steps (5 min each) with PBS with 3% BSA at room temperature followed by 2 washes with PBS, 4',6-diamidino-2-phenylindole (DAPI; Cat# D1306, ThermoFisher Scientific) was added on the cells at 50 ng.mL⁻¹ in PBS and incubated for 10 min at room temperature. Stained cells were washed 3 times in PBS for 5 min at room temperature, and then mounted in Fluoro-gel medium (Cat# 11985-11, Electron Microscopy Sciences, Hatfield, PA) and stored at 4°C

until analysis. Controls with secondary antibody alone without primary antibody did not show any non-specific fluorescent signal. Immunofluorescent micrographs were acquired on an Olympus BX51 microscope with a Hamamatsu C8484 digital camera using a 20× UplanSApo 0.75 numerical aperture objective. The freeware image analysis program Image J (<http://rsb.info.nih.gov/ij/>) was used to generate merged images.

Western blot

Indicated samples were lysed in RIPA buffer (50mM Tris-HCl, pH 7.4, 50 mM NaCl, 2 mM MgCl₂, 1% [vol/vol] NP40, 0.5% [mass/vol] sodium deoxycholate, 0.1% [mass/vol] SDS) as described previously [33,34,31]. The RIPA buffer included freshly added protease inhibitors (Cat# B14002; Biotools, Houston, TX), phosphatase inhibitors (Cat# B15002, Biotools), and benzonase (Cat#71206, Millipore, Billerica, MA). Protein concentrations were determined using the BCA protein assay (Cat# PI23225, Thermo Fisher Scientific, Waltham, MA) and samples were prepared at a 1µg/µl concentration in Laemmli buffer. Indicated samples were loaded on Novex™ WedgeWell™ 4–20% Tris-Glycine Mini Gels, 15-well (Cat# XP04205BOX, Thermo Fisher Scientific, Waltham, MA). Proteins were transferred for 1h at 100 V using TGS (25mM Tris pH=8.5, 192mM glycine, 0.1% (mass/vol) SDS), 20% (vol/vol) methanol as transfer buffer to polyvinylidene difluoride (PVDF) membranes 0.45µm (Cat# IPVH00010, Millipore, Billerica, MA), pre-activated in pure methanol. After transfer, the membranes were blocked at room temperature for 1 hour with TBST (50 mM Tris-HCl, pH 7.4, 150 mM NaCl, 0.1 % Tween 20), 5% (mass/vol) non-fat dry milk, then incubated separately in indicated primary antibodies in TBST, 5% (mass/vol) BSA, overnight at 4°C. Following incubation in horseradish peroxidase-conjugated secondary antibodies from Jackson immunoresearch, blots were revealed by enhanced luminescence (WBKLS0500, Millipore, Billerica, MA) before exposure to photographic film. Films were scanned, digitized, and quantified using Un-Scan-It gel version 6.1 scanning software by Silk Scientific Inc.

Cell proliferation assay

Cell proliferation was analyzed using Click-IT 5-ethynyl-2'-deoxyuridine (EdU; a nucleoside analog of thymidine; Cat# A10044, Thermofisher) at 25µg.mL⁻¹ added 4h before fixation in culture medium. Cells were fixed with pure ice cold methanol, 5min, then dried and stored in PBS at 4°C until use. Either Alexa Fluor 488-azide (Cat# A10266, Thermofisher) or Alexa Fluor 594-Azide (Cat# A10270, Thermofisher) was used in 100mM Tris, 1mM CuSO₄, 100mM ascorbic acid, pH=8.0 for 30min at room temperature, protected from light, to reveal incorporated EdU. Nuclei were stained using DAPI. Immunofluorescent micrographs were acquired on an Olympus BX51 microscope with a Hamamatsu C8484 digital camera using a 20× UplanSApo 0.75 numerical aperture objective. The freeware image analysis program Image J (<http://rsb.info.nih.gov/ij/>) was used to generate images. Analysis was performed by manual of counting EdU stained cells on multiple representative fields to determine proliferation index ratio (EdU/DAPI) in each samples. Results are from 3 independent experiments.

Annexin-V apoptosis assay

Cell apoptosis was analyzed using Annexin V (Cat# A13203, ThermoFisher Scientific) extracellular staining. This stain identifies the phosphatidylserine relocated to the outer leaflet of the plasma membrane in apoptotic conditions. Indicated cells were washed with cold PBS and then incubated in annexin-binding buffer (10 mM HEPES, 140 mM NaCl, and 2.5 mM CaCl₂, pH 7.4) for 15 at room temperature, according to manufacturer's instructions. The cell were washed in cold PBS and then imaged. Analysis was performed by manual counting (by an experimenter blinded to the condition) of highly stained cells from multiple representative fields to determine the percentage of apoptosis in each sample. Results are from 3 independent experiments.

In vivo tumor treatment studies

All procedures and animal care practices were approved and performed in accordance with the Barrow Neurological Institute's Institutional Animal Care and Use Committee.

Tumor Induction

GL261-LucNeo cells were grown in T25 flasks in Dulbecco's modified eagle medium (DMEM) containing glucose, L-glutamine and 10% FBS and supplemented with the aminoglycoside antibiotic G-418 (Geneticin), as a LucNeo selection pressure, at 37°C with 5% CO₂ and maintained under normal adherent culture conditions. Cells were collected with 0.25% trypsin-EDTA, and a Cellometer mini (Nexcelom Bioscience, Lawrence, MA USA) was used to count cells. Orthotopic GL261-LucNeo tumors were induced in C57BL/6 albino mice (25–30g, Charles River) as previously reported [35–37]. Briefly, mice were anesthetized with an intraperitoneal (i.p.) injection of ketamine/xylazine (100/10 mg/kg) prior to being mounted in a stereotaxic frame (Kopf Instruments, Tujunga, CA, USA) on top of an infrared heating pad to maintain animal temperature. The animal's head was shaved and sterilized with three alternating passes of each betadine and ethanol. A 1 cm incision was made over midline, and a burr hole was drilled 2 mm lateral, 0.1 mm posterior of bregma. A Hamilton syringe (29 gauge needle) containing 75,000 GL261-LucNeo cells in 2 µl DMEM was inserted into the hole to a depth of 2.8 mm and the cells were injected over 2 min. The needle was left in place for 1 min to reduce backflow before the wound was closed with staples. All animals received a subcutaneous (SQ) injection of buprenorphine sustained-release formulation prior to surgery, and ibuprofen was provided in their water *ad libitum* for 1 week for pain.

Immunohistofluorescence and epifluorescence imaging

Mouse brains injected with GL261 cells (at day 17 post injection) were perfused using 4% paraformaldehyde. They were next transferred into a 30% sucrose solution and left at 4°C until the sinking of the tissues could be observed (~3 days). Tissues were cut at 10 µm thickness using the Bright OTF 5000 Microtome Cryostat (Hacker Instruments and Industries, Inc., Winnsboro, SC), and fixed onto gelatin coated glass slides and kept at –20°C until use. Brain slices were permeabilized and saturated using PBS containing 3% BSA, 0.1% triton X-100 solution for 30 min at RT, and then antibodies were added overnight. The antibodies used were: CRMP2 (Cat#C2993, Sigma, St Louis, MO or

Cat#11096, Immuno-Biological Laboratories, Minneapolis, USA); CRMP2 pSer522 (Cat#CP2191, ECM Biosciences, Versailles, KY). The slices were then washed 3X in PBS, and incubated with PBS containing 3% BSA, 0.3% triton X-100 containing secondary antibodies (Alexa 488 goat anti-rabbit secondary antibody (Life Technologies)) for at least 3 hrs at RT. After 3 washes (PBS, 10 min, RT), either DAPI was used to stain the nuclei of cells. Slides were mounted and stored at 4°C until analysis. Immunofluorescent micrographs were acquired on an Olympus BX51 microscope with a Hamamatsu C8484 digital camera using a 4× UplanFL N, 0.13 numerical aperture or a 20× UplanSApo 0.75 numerical aperture objective. The freeware image analysis program Image J (<http://rsb.info.nih.gov/ij/>) was used to generate merged images.

Tumor Growth

Bioluminescence was used to monitor and measure tumor growth as previously described [35,37]. Imaging was done on the Xenogen IVIS Spectrum *in vivo* imaging system every 3–4 days starting 6 days after tumor implantation. Luciferin (150 mg/kg) was administered SQ and the mice were imaged 25 min later under 2% isoflurane. The Living Image software was used to draw an ROI around the tumor signal and measure the size of each tumor (total flux, photons/sec).

Tumor Treatment

Mice were randomly assigned to a treatment group, saline or (S)-Lacosamide (30 mg/kg, i.p.), after the first imaging session (day 6). Treatments were administered daily by intraperitoneal (i.p.) injection for 10 days beginning on day 7 post tumor induction. Therapeutic efficacy was evaluated by measuring tumor growth via bioluminescence. Mice were monitored daily for signs of neurological symptoms (lack of grooming, abnormal gait, hunched posture etc.) or greater than 15% weight loss. Investigators were blinded to the treatment condition.

Data analysis

All data columns are shown as mean \pm S.E.M. In Western blots, n is presented as the number of separate experiments (minimum of 3). Western blots were quantified using Un-Scan-It gel version 6.1 (Silk Scientific Inc., Orem, UT). Statistical differences between control and experimental conditions were determined by using Mann Whitney non-parametric test followed by Dunnet's post hoc test or a Mann & Whitney non-parametric test when comparing only two conditions within R Software (R-project). P values < 0.05 were judged to be statistically significant. Graphs were generated using Graphpad Prism 7 software.

Results

Neurofibromin expression levels correlate with CRMP2 phosphorylation levels in glioblastoma

In glioblastoma, loss of neurofibromin, the protein product of the *nf1* gene, is a marker of poor survival and resistance to treatments [5,6]. This loss results in dysregulation of neurofibromin interacting proteins including the oncogene Ras [11] and CRMP2 [17]. The interaction between CRMP2 and neurofibromin results in inhibition of CRMP2

phosphorylation by Cdk5 [17]. Notably, CRMP2 phosphorylation, but not expression, levels have been positively linked to cancer progression [18,19]. Thus, we investigated the correlation between CRMP2 expression and phosphorylation levels with neurofibromin expression in glioblastoma. We used three different human GBM cell lines to account for the very high heterogeneity of the tumors [10]. By western blot analysis, we first characterized neurofibromin expression in the three different GBM cell lines (Fig. 1A). Although all three cell lines had detectable neurofibromin levels, we found that the U87 cells had the highest level of neurofibromin expression ($253 \% \pm 12.1$ compared to GL15 cell level, $p < 0.0001$, Kruskal-Wallis test), A172 cells had the lowest expression of neurofibromin ($66 \% \pm 5.5$ compared to GL15 cell level, $p < 0.041$, Kruskal-Wallis test) (Fig. 1A, B). We next examined CRMP2 expression levels in the three GBM cell lines and found that CRMP2 expression was highest in U87 ($282.4 \% \pm 7.1$, $p < 0.0001$, Kruskal-Wallis test) and lowest in A172 ($58 \% \pm 5.5$, $p < 0.0109$, Kruskal-Wallis test) cells compared to GL15 cells (Fig. 1A, B). Finally, we analyzed CRMP2 phosphorylation by Cdk5 levels using an antibody specific to the S522 phosphorylation site on CRMP2. The phosphorylated CRMP2 signal was normalized to CRMP2 expression level for each cell line. We found that CRMP2 phosphorylation at the S522 site was increased in A172 cells ($142 \% \pm 4.4$, $p < 0.011$, Kruskal-Wallis test) and decreased in U87 cells ($64 \% \pm 6.7$, $p < 0.0333$, Kruskal-Wallis test) compared to levels in GL15 cells (Fig. 1A, B). These results highlight the differential expression of neurofibromin, CRMP2 and phosphorylated CRMP2 in glioblastoma. Since CRMP2's interaction with neurofibromin results in inhibition of CRMP2 phosphorylation, we asked if neurofibromin levels would be correlated with CRMP2 phosphorylation levels. Using a Pearson correlation analysis from our western blot data (Fig. 1A, B), we found that the more neurofibromin levels correlated inversely with phosphorylated CRMP2 (S522) levels in GBM cells (Fig. 1C) ($r^2 = 0.85$, $p < 0.0094$). Thus, in the glioblastoma lines tested here, less neurofibromin, an event linked to poor survival [5,6], leads to more CRMP2 phosphorylation.

Phosphorylated CRMP2 is localized in the nucleus of glioblastoma cells

Previous studies have shown that subcellular localization of phosphorylated CRMP2 is altered in cancer cells [21,18]. Thus, we examined localization of CRMP2 and phosphorylated CRMP2 in glioblastoma cells using fluorescent immunostaining. We detected total CRMP2 in both the cytoplasm and the nucleus of the three GBM cell lines (Fig. 2, top panels). In contrast, phosphorylated CRMP2 (S522), was only detected in the nucleus of the three GBM cell lines (Fig. 2, bottom panels). These results show that CRMP2 phosphorylation (S522) is relocalized in the nucleus of GBM cells. Such nuclear localization for CRMP2 was described previously in lung cancer and was suggested to have a role in cell proliferation [21].

CRMP2 expression participates in glioblastoma cell proliferation

CRMP2 expression in glioblastoma and its localization in the cytoplasm and in the nucleus, suggests a role for this protein in this tumor. In glioblastoma, the fast growing behavior of the tumors likely accounts for the lower survival of patients [23]. To assess the contribution of CRMP2 to the proliferation of glioblastoma cell lines, we used a genetic knockdown strategy. Using short interfering RNAs (siRNAs), we knocked down CRMP2 by ~50% in all

cell lines (Fig. 3A, B). We then performed a 5-ethynyl-2'-deoxyuridine (EdU) incorporation assay to evaluate the contribution of CRMP2 expression to glioblastoma cell proliferation (Fig. 3C). Following CRMP2 knockdown, the proliferation ratio was decreased in all three cell lines: GL15 ($22.7\% \pm 1.55$ compared to control, $p < 0.0001$, Mann Whitney test), A172 ($20\% \pm 4$ compared to control, $p < 0.0001$, Mann Whitney test) and U87 ($39.4\% \pm 8.4$ compared to control, $p < 0.0001$, Mann Whitney test). These results demonstrate an important role for CRMP2 in glioblastoma proliferation.

CRMP2 expression and phosphorylation control glioblastoma cell proliferation

Having demonstrated that CRMP2 levels contribute to GBM proliferation, we next asked if CRMP2 phosphorylation could be the event driving GBM proliferation. To answer this, we used phospho-deficient CRMP2 constructs mutated on either the phosphorylation site for Cdk5 (S522A) or the phosphorylation sites for Glycogen synthase kinase 3 beta (GSK3 β) (T509A/T514A); GSK3 β mediated phosphorylation of CRMP2 occurs following the priming phosphorylation event by Cdk5 [38]. Since the plasmids used in this study allow expression of CRMP2 fused to a dsRed fluorescent tag to identify the transfected cells, we were able to quantify EdU incorporation signal in only the dsRed positive (i.e., transfected) cells (Fig. 4A). We found a differential contribution of CRMP2 and phospho-deficient CRMP2 to GBM cell proliferation in the three cell lines used. CRMP2 overexpression increased the proliferation, compared to dsRed expression, of A172 ($169.1\% \pm 23.3$, $p < 0.01$, Kruskal-Wallis test) and U87 ($188.6\% \pm 10.1$, $p < 0.001$, Kruskal-Wallis test) but not of the GL15 cells (Fig. 4B). Expressing a CRMP2 that cannot be phosphorylated by Cdk5 (S522A), decreased the proliferation, compared to dsRed expression, of GL15 ($38\% \pm 4.9$, $p < 0.05$, Kruskal-Wallis test) and A172 ($55\% \pm 16$, $p < 0.05$, Kruskal-Wallis test) cells but not U87 cells (Fig. 4B). Of note here, expressing CRMP2-S522A in U87 cells prevented the increase of proliferation observed when wildtype CRMP2 was expressed (Fig. 4B). Finally, when we expressed a CRMP2 that cannot be phosphorylated by GSK3 β (T509A/T514A), the proliferation, compared to dsRed expression, was decreased only in A172 ($42.6\% \pm 13$, $p < 0.05$, Kruskal-Wallis test) cells (Fig. 4B). Again, in U87 cells, expressing CRMP2 T509A/T514A prevented the increase of proliferation observed when wildtype CRMP2 was expressed (Fig. 4B). No significant effect of CRMP2 T509A/T514A expression was observed in GL15 cells. These results show: (i) CRMP2 expression can increase GBM cell proliferation, and (ii) CRMP2 phosphorylation at S522 is an important phosphorylation event for CRMP2 that drives GBM cell proliferation.

(S)-Lacosamide inhibits CRMP2 phosphorylation in GBM cell lines

To explore further the role of CRMP2 phosphorylation at S522 in glioblastoma, we used the CRMP2 phosphorylation inhibitor (*S*)-lacosamide. (*S*)-lacosamide is a small molecule that we previously identified as a specific inhibitor of CRMP2 phosphorylation by Cdk5 in both central nervous system (CNS) [27] and peripheral nervous system (PNS)[26,25] neurons. Prior to using this compound for functional assays, we wanted to control its efficiency in inhibiting CRMP2 phosphorylation in human GBM cell lines. The cells were seeded at 70% confluence and treated 24h after seeding to capture their exponential growing phase. (*S*)-lacosamide was applied at 2, 20 or 200 μM overnight and then the cells were harvested and processed for western blotting. We probed the samples for total CRMP2 and CRMP2

phosphorylated by Cdk5 (pS522) (Fig. 5A). The pS522 signal was quantified and normalized to the total CRMP2 signal. We observed a concentration-dependent inhibition of CRMP2 phosphorylation (S522) when the cells were treated with (*S*)-lacosamide. These results show the efficiency of (*S*)-lacosamide to inhibit CRMP2 phosphorylation (S522) in GBM cell lines. Thus, this compound can be used to interrogate the functional consequence of CRMP2 phosphorylation in glioblastoma cells.

Inhibiting CRMP2 phosphorylation with (*S*)-lacosamide decreases GBM cell proliferation

So far, our results demonstrate that GBM cell proliferation is under the control of CRMP2 expression levels: knocking down CRMP2 decreased the proliferation of three GBM cell lines (Fig. 3) while overexpressing CRMP2 increased the proliferation of A172 and U87 GBM cell lines (Fig. 4). Also, expressing a phospho-deficient CRMP2 that cannot be phosphorylated resulted in decreased proliferation of GL15 and A172 GBM cell lines and prevented the CRMP2-dependent increase of proliferation in U87 cells (Fig. 4). These results show that CRMP2 phosphorylation (S522) is a major determinant of GBM cell proliferation. To investigate the contribution of CRMP2 phosphorylation at S522 to cancer cell proliferation, we used the CRMP2 phosphorylation inhibitor (*S*)-lacosamide. We seeded cells at 70% confluence and treated 24 h after seeding to capture their exponential growing phase. (*S*)-lacosamide was applied at 2, 20 or 200 μM overnight and EdU applied during 4 hours before fixation. We quantified the proliferation ratio (EdU/DAPI) of the cells treated as described (Fig. 6A). We found that inhibiting CRMP2 phosphorylation with (*S*)-lacosamide decreased glioblastoma cell proliferation in all GBM cell lines (Fig. 6A,B). The maximum reduction of the proliferation ratio was achieved at a 200 μM concentration of (*S*)-lacosamide, compared to the control (0.04% DMSO) in GL15 ($42.3\% \pm 2.47$, $p < 0.001$, Kruskal-Wallis test), A172 ($40.8\% \pm 1.88$, $p < 0.001$, Kruskal-Wallis test) and U87 ($22.1\% \pm 1.49$, $p < 0.001$, Kruskal-Wallis test) cells (Fig. 6B). Thus, inhibiting CRMP2 phosphorylation using (*S*)-lacosamide results in a concentration-dependent decrease of GBM cell proliferation.

In a previous study linking CRMP2 phosphorylation to cancer progression, expressing a phospho-deficient CRMP2 resulted in increased apoptosis of lung cancer cells [21]. Thus, to assess the contribution of CRMP2 phosphorylation in glioblastoma cell survival, we used (*S*)-lacosamide to inhibit CRMP2 phosphorylation and assessed the apoptosis rate of the GBM cells using extracellular Annexin-V staining. Annexin V is commonly used to detect apoptotic cells by its ability to bind to phosphatidylserine, a marker of apoptosis when it is on the outer leaflet of the plasma membrane. In GL15 cells, the apoptosis rate reached 100% when the cells were treated with 200 μM of (*S*)-lacosamide (Fig. 6C). The A172 cells showed a lower basal apoptosis rate ($11.7\% \pm 3$ in untreated cells), which increased to $80.1\% \pm 6.5$ when the cells were treated with 200 μM of (*S*)-lacosamide (Fig. 6C). The U87 cells had the lowest increase of apoptosis between the control treatment ($39.8\% \pm 6.6$) and the 200 μM (*S*)-lacosamide treatment ($72.3\% \pm 7.6$) (Fig. 6C). Taken together, these results underscore the importance of CRMP2 phosphorylation at S522, as a major regulator of GBM cell proliferation and as a negative regulator of apoptosis.

(S)-lacosamide inhibits glioblastoma growth in vivo

We have shown that CRMP2 expression and phosphorylation controls GBM cell proliferation in vitro. (S)-lacosamide, a CRMP2 phosphorylation inhibitor, inhibited the proliferation of three GBM cell lines and induced apoptosis in these cells. (S)-lacosamide is a relatively brain permeable compound with a measured brain-to-plasma partition coefficient of 0.55 [39]. Thus, we next asked if (S)-lacosamide could affect GBM growth in vivo. We used the murine GL261 in vivo GBM model that recapitulates key features found in human tumors, namely the invasive properties, high proliferation, active angiogenesis, necrosis, hypoxic zones and impairment of the blood-brain barrier [29,40]. Tumors were induced in immunocompetent mice by stereotaxic injection of 75,000 GL261-LucNeo cells into the right striatum. In these cells CRMP2 is expressed throughout the cytoplasm while pS522-CRMP2 is largely restricted to the nucleus (Fig. 7A). Importantly, this cell model allows the tumor to grow within an appropriate brain microenvironment to better mimic human disease. Tumors elicit detectable bioluminescence signal soon after induction due to peroxidation of luciferin (administered 150 mg/kg, i.p.) by luciferase expressed by the GL261-LucNeo cells, which enables monitoring of tumor growth and response to treatment via bioluminescent imaging. At day 7, (S)-lacosamide (30 mg/kg) or saline (vehicle) was administered daily by i.p. injections and the tumor growth was followed for 10 days (Fig. 7B). After 10 days of daily treatments with (S)-lacosamide, we observed a ~47% decrease in tumor size ($0.79 \times 10^7 \pm 0.16 \times 10^7$) relative to vehicle treated animals ($1.7 \times 10^7 \pm 0.5 \times 10^7$); although the group sizes were relatively small, these differences in tumor growth were statistically significant at day 17 ($p < 0.02$, Sidak's correction for multiple comparisons applied to a two-way repeat measure ANOVA, $n = 5$ mice per group) (Fig. 7C). This suggests that the (S)-lacosamide treatment decreased GBM growth in vivo. To better assess the overall growth decrease resulting from (S)-lacosamide treatment, we calculated the area under the curve between day 10 (to allow time for (S)-lacosamide to start being effective) and day 17. We found a decreased area under the curve (~54%) when the animals were treated with (S)-lacosamide ($1.7 \times 10^7 \pm 0.3 \times 10^7$) compared to vehicle treated animals ($3.8 \times 10^7 \pm 0.8 \times 10^7$), which was also a significant difference ($p < 0.05$, two-tailed Student's t test) (Fig. 7D). These results provide evidence that the CRMP2 phosphorylation inhibitor (S)-lacosamide affects the growth of GBM vivo.

Discussion

The discovery reported here is important from a fundamental scientific perspective because a knowledge gap in the pro-oncogenic mechanism of glioblastoma is filled. It is also important from an applied perspective because glioblastoma remains a significant unmet clinical need. Our study identifies the contribution of CRMP2 expression and phosphorylation to glioblastoma proliferation in vitro and growth in vivo, thus introducing a novel protein contributing to glioblastoma oncogenic mechanisms. We found a negative correlation between CRMP2 phosphorylation and neurofibromin expression in vitro across three human GBM cell lines. We demonstrated that GBM cell proliferation was dependent on CRMP2 expression and phosphorylation at S522. We next used the small molecule (S)-lacosamide to inhibit CRMP2 phosphorylation, inhibit proliferation and induce apoptosis in three GBM

cell lines. (S)-lacosamide was also able to decrease orthotopic GBM growth, thus showing the importance of CRMP2 phosphorylation for GBM proliferation *in vivo*.

Glioblastoma tumors have been classified, based on their molecular signatures, into four different subtypes including, proneural, neural, classical and mesenchymal [3]. In this study, expression of CRMP2 transcripts was detected but not linked to a particular subtype or to patient's survival [23]. However, messenger RNA expression does not necessarily correlate with protein expression and does not account for CRMP2 post-translational modification status. A recent clustered regularly interspaced short palindromic repeats (CRISPR) screen identified several novel mediators of glioblastoma survival outside of the commonly altered molecular networks [41]. In this high-throughput study, deleting CRMP2 had a negative effect on the survival of the GBM cells tested [41], in agreement with our data showing the contribution of CRMP2 expression to GBM cell proliferation.

We recently highlighted the role that different CRMP2 post-translational modifications play in determining the cellular functions served by CRMP2 [31]. CRMP2 phosphorylation by Cdk5 was found to control CRMP2 subsequent phosphorylation by GSK3 β [42] and SUMOylation (addition of small ubiquitin like modifier (SUMO)) by the E2 ubiquitin-conjugating enzyme Ubc9 [31]. Cdk5 phosphorylation of CRMP2 is resistant to dephosphorylation [43] but can be removed by decreasing the stability of the protein [44]. This particular phosphorylation of CRMP2 has been reported to be associated with cancer progression [18,19]. Here, we extended these findings to GBM and distinctively demonstrate a rapidly observable functional requirement of CRMP2 phosphorylation for glioblastoma proliferation and survival. Expressing a CRMP2-deficient for GSK3 β phosphorylation, but not for Cdk5 phosphorylation, decreased GBM cell proliferation in two of the cell lines tested. Thus, we conclude that the GSK3 β phosphorylation site in CRMP2 is important for glioblastoma cell proliferation. Additionally, CRMP2 phosphorylation at S522 might serve as a hub, enabling novel downstream signaling pathways to regulate CRMP2 and drive the protein into different cellular functions such as cancer cell proliferation or chronic pain [45]. GSK3 β is a well-known mediator of glioblastoma growth [46] and resistance to treatments [47,48]. Our data point to CRMP2 as a possible molecular target downstream of GSK3 β and thus likely to be associated with GBM recurrence. Although CRMP2 phosphorylation at S522 by Cdk5 has been previously reported [18], we cannot rule out the possibility that an unknown kinase(s) may phosphorylate CRMP2 at this site within the GBM.

The mechanism by which CRMP2 promotes cell proliferation and survival is an open question. A previous study linked CRMP2 phosphorylation by Cdk5 to different phases of mitosis [21]. Overexpressing CRMP2 showed a trend towards a faster mitotic cycle. However, expressing a CRMP2 deficient for Cdk5 phosphorylation prevented this effect. Cells expressing a phospho-deficient CRMP2, accumulated in the telophase phase of mitosis [21]. This event preceding cytokinesis relies on extensive microvesicle trafficking [49] and molecule interacting with CasL 1 (MICAL1) enzymatic activity [50], two events linked to CRMP2 phosphorylation. A separate study demonstrated CRMP2 phosphorylation by Cdk5 to be an important mediator of ion channel trafficking [27,31,51]. Thus, CRMP2 phosphorylation by Cdk5 might be required during cytokinesis to mediate microvesicle trafficking. CRMP2 phosphorylation by Cdk5 and GSK3 β is triggered by Semaphorin 3A

signaling [52]. However, MICAL1 autoinhibition is released by an interaction with CRMP proteins under Semaphorin 3A stimulation [53]. These studies triangulate to link the increased CRMP2 phosphorylation in glioblastoma to facilitated cytokinesis through increased microvesicle trafficking and MICAL1 enzymatic activity. This is further supported by the finding that glioblastoma displays an autocrine semaphorin 3A signaling [54] which can contribute to promoting sustained proliferation through induction of CRMP2 phosphorylation. Another aspect of CRMP2 contribution to glioblastoma growth and survival could be through forward trafficking of channels and/or receptors. We recently reported CRMP2-mediated internalization of a sodium channel via a clathrin-dependent endocytosis mechanism through interactions with the endocytic adaptor Numb [31]. Numb is a protein mediating the endocytosis of the epidermal growth factor receptor (EGFR) [55]. Activating mutations (EGFR vIII) or copy number amplifications of EGFR gene are highly incident in human glioblastoma tumors (gene mutated in 57% of cases [2] and amplified in 84% of cases [3]). When phosphorylated by Cdk5, CRMP2 loses its interaction with Numb which results in ion channel clathrin-mediated endocytosis defects [31]. These findings lend support to the hypothesis that the increased CRMP2 phosphorylation at S522 in glioblastoma could further amplify EGFR signaling leading to sustained tumor cell proliferation and resistance.

We found CRMP2 phosphorylation levels to be inversely correlated with neurofibromin expression level across three GBM cell lines. Although the neurofibromin status of GL15 cells is not known, A172 and U87 cells were reported to express neurofibromin [56]. Our results showed the role of CRMP2 phosphorylation in glioblastoma cell proliferation but, interestingly, it was the neurofibromin expression level in each cell line that defined their response to loss of CRMP2 phosphorylation. The only cell line where the expression of phospho-deficient CRMP2 did not result in a decrease of proliferation compared to the control was U87. This cell line had the highest expression of neurofibromin and the lowest level of CRMP2 phosphorylation. Similarly, the cell line that was the most impacted by our manipulations of CRMP2 expression and phosphorylation was A172. This cell line had the lowest level of neurofibromin and the highest level of phosphorylated CRMP2. These observations translated when we used (*S*)-lacosamide and U87 cells showed a decrease of proliferation only at the highest concentration of the compound. This was linked with a less pronounced increase in apoptosis compared to the two other cell lines. These observations show that under neurofibromin loss, phosphorylated CRMP2 becomes an important determinant of glioblastoma proliferation and survival.

CRMP2 phosphorylation by GSK3 β appears to be an important determinant of glioblastoma proliferation and survival. GSK3 β inhibition using lithium chloride has been reported to be beneficial in inhibiting glioblastoma growth and inducing apoptosis [57]. A limitation of potential therapeutic inhibition of GSK3 β is that such inhibiting GSK3 β will, in turn, activate the Wnt signaling pathway by protecting β -catenin from degradation. The Wnt signaling pathway promotes the maintenance of a cancer stem cell pool in glioblastoma, which will contribute to tumor recurrence after treatment, leading to future resistance [58]. In this regard, inhibiting the phosphorylation of GSK3 β 's downstream targets, instead of the kinase itself, may be a viable alternative strategy. We used (*S*)-lacosamide to inhibit CRMP2 phosphorylation in three GBM cell lines. This resulted in an inhibition of cell proliferation

and induced apoptosis in these cells. Subjects bearing orthotopic GBM and treated with (*S*)-lacosamide showed evidence for a slowing of tumor growth compared to saline treated controls, thus implicating that CRMP2 phosphorylation is driving GBM growth. This result also showed that targeting CRMP2 phosphorylation could be beneficial, in combination with other therapeutic approaches, to treat GBM; future studies will be needed to rigorously test this hypothesis. Because GL261 cells used in our tumor model have been reported to contain CD133+ (cancer stem-like cells) and CD133- cells [59], a potential limitation of our study is that this we cannot cellular heterogeneity is likely to impact the effect of (*S*)-LCM.

Taken together, our data introduce CRMP2 expression and phosphorylation as important molecular events driving glioblastoma proliferation and survival in vitro and in vivo. Our use of (*S*)-lacosamide illustrates repurposing of an inactive anti-epileptic molecule for probing of CRMP2 phosphorylation functions in brain tumors. (*S*)-LCM does not impair motor performance or elicit other observable side-effects in rodents [60]. If this molecule exhibits appropriate drug-like qualities, like its R-isomer (Vimpat®), additional efficacy and safety evaluation could facilitate translation of (*S*)-lacosamide or other molecules targeting CRMP2 phosphorylation into new therapeutic strategies to treat GBM in the clinic.

Acknowledgments

This work was supported by a Neurofibromatosis New Investigator Award from the Department of Defense Congressionally Directed Military Medical Research and Development Program (NF1000099) and a Children's Tumor Foundation NF1 Synodos award to R.K. A.M. was supported by a Young Investigator's Award from the Children's Tumor Foundation. L.S.V. was supported by grants from a T35 HL07479-31A1 training grant from the NIH/NHLBI to Marlys H. Witte (Department of Surgery, University of Arizona) as well as a grant from the Undergraduate Biology Research Program (UBRP), University of Arizona and Western Alliance to Expand Student Opportunities (WAESO) Louis Stokes Alliance for Minority Participation (LSAMP) National Science Foundation (NSF) Cooperative Agreement No. HRD-1101728. Further support was provided by Arizona State University (K.T.H.) and the Barrow Neurological Foundation (K.T.H., R.W.S.)

References

1. Stupp R, Mason WP, van den Bent MJ, Weller M, Fisher B, Taphoorn MJ, Belanger K, Brandes AA, Marosi C, Bogdahn U, Curschmann J, Janzer RC, Ludwin SK, Gorlia T, Allgeier A, Lacombe D, Cairncross JG, Eisenhauer E, Mirimanoff RO, European Organisation for R, Treatment of Cancer Brain T, Radiotherapy G, National Cancer Institute of Canada Clinical Trials G. Radiotherapy plus concomitant and adjuvant temozolomide for glioblastoma. *N Engl J Med*. 2005; 352(10):987–996. DOI: 10.1056/NEJMoa043330 [PubMed: 15758009]
2. Brennan CW, Verhaak RG, McKenna A, Campos B, Noushmehr H, Salama SR, Zheng S, Chakravarty D, Sanborn JZ, Berman SH, Beroukhi R, Bernard B, Wu CJ, Genovese G, Shmulevich I, Barnholtz-Sloan J, Zou L, Vegesna R, Shukla SA, Ciriello G, Yung WK, Zhang W, Sougnez C, Mikkelsen T, Aldape K, Bigner DD, Van Meir EG, Prados M, Sloan A, Black KL, Eschbacher J, Finocchiaro G, Friedman W, Andrews DW, Guha A, Iacocca M, O'Neill BP, Foltz G, Myers J, Weisenberger DJ, Penny R, Kucherlapati R, Perou CM, Hayes DN, Gibbs R, Marra M, Mills GB, Lander E, Spellman P, Wilson R, Sander C, Weinstein J, Meyerson M, Gabriel S, Laird PW, Haussler D, Getz G, Chin L, Network TR. The somatic genomic landscape of glioblastoma. *Cell*. 2013; 155(2):462–477. DOI: 10.1016/j.cell.2013.09.034 [PubMed: 24120142]
3. Verhaak RG, Hoadley KA, Purdom E, Wang V, Qi Y, Wilkerson MD, Miller CR, Ding L, Golub T, Mesirov JP, Alexe G, Lawrence M, O'Kelly M, Tamayo P, Weir BA, Gabriel S, Winckler W, Gupta S, Jakkula L, Feiler HS, Hodgson JG, James CD, Sarkaria JN, Brennan C, Kahn A, Spellman PT, Wilson RK, Speed TP, Gray JW, Meyerson M, Getz G, Perou CM, Hayes DN, Cancer Genome Atlas Research N. Integrated genomic analysis identifies clinically relevant subtypes of

- glioblastoma characterized by abnormalities in PDGFRA, IDH1, EGFR, and NF1. *Cancer Cell*. 2010; 17(1):98–110. DOI: 10.1016/j.ccr.2009.12.020 [PubMed: 20129251]
4. Bianco J, Bastiancich C, Jankovski A, des Rieux A, Preat V, Danhier F. On glioblastoma and the search for a cure: where do we stand? *Cell Mol Life Sci*. 2017; doi: 10.1007/s00018-017-2483-3
 5. Parsons DW, Jones S, Zhang X, Lin JC, Leary RJ, Angenendt P, Mankoo P, Carter H, Siu IM, Gallia GL, Olivi A, McLendon R, Rasheed BA, Keir S, Nikolskaya T, Nikolsky Y, Busam DA, Tekleab H, Diaz LA Jr, Hartigan J, Smith DR, Strausberg RL, Marie SK, Shinjo SM, Yan H, Riggins GJ, Bigner DD, Karchin R, Papadopoulos N, Parmigiani G, Vogelstein B, Velculescu VE, Kinzler KW. An integrated genomic analysis of human glioblastoma multiforme. *Science*. 2008; 321(5897): 1807–1812. DOI: 10.1126/science.1164382 [PubMed: 18772396]
 6. Sintupisut N, Liu PL, Yeang CH. An integrative characterization of recurrent molecular aberrations in glioblastoma genomes. *Nucleic acids research*. 2013; 41(19):8803–8821. DOI: 10.1093/nar/gkt656 [PubMed: 23907387]
 7. Plaisier CL, O'Brien S, Bernard B, Reynolds S, Simon Z, Toledo CM, Ding Y, Reiss DJ, Paddison PJ, Baliga NS. Causal Mechanistic Regulatory Network for Glioblastoma Deciphered Using Systems Genetics Network Analysis. *Cell Syst*. 2016; 3(2):172–186. DOI: 10.1016/j.cels.2016.06.006 [PubMed: 27426982]
 8. Wood MD, Reis GF, Reuss DE, Phillips JJ. Protein Analysis of Glioblastoma Primary and Posttreatment Pairs Suggests a Mesenchymal Shift at Recurrence. *J Neuropathol Exp Neurol*. 2016; 75(10):925–935. DOI: 10.1093/jnen/nlw068 [PubMed: 27539476]
 9. Lu KV, Chang JP, Parachoniak CA, Pandika MM, Aghi MK, Meyronet D, Isachenko N, Fouse SD, Phillips JJ, Cheresch DA, Park M, Bergers G. VEGF inhibits tumor cell invasion and mesenchymal transition through a MET/VEGFR2 complex. *Cancer Cell*. 2012; 22(1):21–35. DOI: 10.1016/j.ccr.2012.05.037 [PubMed: 22789536]
 10. Sottoriva A, Spiteri I, Piccirillo SG, Touloumis A, Collins VP, Marioni JC, Curtis C, Watts C, Tavaré S. Intratumor heterogeneity in human glioblastoma reflects cancer evolutionary dynamics. *Proceedings of the National Academy of Sciences of the United States of America*. 2013; 110(10): 4009–4014. DOI: 10.1073/pnas.1219747110 [PubMed: 23412337]
 11. Ballester R, Marchuk D, Boguski M, Saulino A, Letcher R, Wigler M, Collins F. The NF1 locus encodes a protein functionally related to mammalian GAP and yeast IRA proteins. *Cell*. 1990; 63(4):851–859. [PubMed: 2121371]
 12. McGillicuddy LT, Fromm JA, Hollstein PE, Kubek S, Beroukhir R, De Raedt T, Johnson BW, Williams SM, Nghiemphu P, Liau LM, Cloughesy TF, Mischel PS, Parret A, Seiler J, Moldenhauer G, Scheffzek K, Stemmer-Rachamimov AO, Sawyers CL, Brennan C, Messiaen L, Mellinghoff IK, Cichowski K. Proteasomal and genetic inactivation of the NF1 tumor suppressor in gliomagenesis. *Cancer Cell*. 2009; 16(1):44–54. DOI: 10.1016/j.ccr.2009.05.009 [PubMed: 19573811]
 13. Zuckermann M, Hovestadt V, Knobbe-Thomsen CB, Zapatka M, Northcott PA, Schramm K, Belic J, Jones DT, Tschida B, Moriarity B, Largaespada D, Roussel MF, Korshunov A, Reifenberger G, Pfister SM, Lichter P, Kawachi D, Gronych J. Somatic CRISPR/Cas9-mediated tumour suppressor disruption enables versatile brain tumour modelling. *Nature communications*. 2015; 6:7391. doi: 10.1038/ncomms8391
 14. Goshima Y, Nakamura F, Strittmatter P, Strittmatter SM. Collapsin-induced growth cone collapse mediated by an intracellular protein related to UNC-33. *Nature*. 1995; 376(6540):509–514. DOI: 10.1038/376509a0 [PubMed: 7637782]
 15. Fukata Y, Itoh TJ, Kimura T, Menager C, Nishimura T, Shiromizu T, Watanabe H, Inagaki N, Iwamatsu A, Hotani H, Kaibuchi K. CRMP-2 binds to tubulin heterodimers to promote microtubule assembly. *Nature cell biology*. 2002; 4(8):583–591. DOI: 10.1038/ncb825 [PubMed: 12134159]
 16. Ip JP, Fu AK, Ip NY. CRMP2: Functional Roles in Neural Development and Therapeutic Potential in Neurological Diseases. *The Neuroscientist : a review journal bringing neurobiology, neurology and psychiatry*. 2014; doi: 10.1177/1073858413514278
 17. Patrakitkomjorn S, Kobayashi D, Morikawa T, Wilson MM, Tsubota N, Irie A, Ozawa T, Aoki M, Arimura N, Kaibuchi K, Saya H, Araki N. Neurofibromatosis type 1 (NF1) tumor suppressor, neurofibromin, regulates the neuronal differentiation of PC12 cells via its associating protein,

- CRMP-2. *The Journal of biological chemistry*. 2008; 283(14):9399–9413. DOI: 10.1074/jbc.M708206200 [PubMed: 18218617]
18. Grant NJ, Coates PJ, Woods YL, Bray SE, Morrice NA, Hastie CJ, Lamont DJ, Carey FA, Sutherland C. Phosphorylation of a splice variant of collapsin response mediator protein 2 in the nucleus of tumour cells links cyclin dependent kinase-5 to oncogenesis. *BMC Cancer*. 2015; 15:885.doi: 10.1186/s12885-015-1691-1 [PubMed: 26555036]
 19. Tan F, Thiele CJ, Li Z. Collapsin response mediator proteins: Potential diagnostic and prognostic biomarkers in cancers (Review). *Oncol Lett*. 2014; 7(5):1333–1340. DOI: 10.3892/ol.2014.1909 [PubMed: 24765134]
 20. Shimada K, Ishikawa T, Nakamura F, Shimizu D, Chishima T, Ichikawa Y, Sasaki T, Endo I, Nagashima Y, Goshima Y. Collapsin response mediator protein 2 is involved in regulating breast cancer progression. *Breast Cancer*. 2014; 21(6):715–723. DOI: 10.1007/s12282-013-0447-5 [PubMed: 23381229]
 21. Oliemuller E, Pelaez R, Garasa S, Pajares MJ, Agorreta J, Pio R, Montuenga LM, Teijeira A, Llanos S, Rouzaut A. Phosphorylated tubulin adaptor protein CRMP-2 as prognostic marker and candidate therapeutic target for NSCLC. *Int J Cancer*. 2013; 132(9):1986–1995. DOI: 10.1002/ijc.27881 [PubMed: 23023514]
 22. Mukherjee J, DeSouza LV, Micallef J, Karim Z, Croul S, Siu KW, Guha A. Loss of collapsin response mediator Protein1, as detected by iTRAQ analysis, promotes invasion of human gliomas expressing mutant EGFRvIII. *Cancer Res*. 2009; 69(22):8545–8554. DOI: 10.1158/0008-5472.CAN-09-1778 [PubMed: 19903856]
 23. Moutal A, Honnorat J, Massoma P, Desormeaux P, Bertrand C, Malleval C, Watrin C, Chounlamountri N, Mayeur ME, Besancon R, Naudet N, Magadoux L, Khanna R, Ducray F, Meyronet D, Thomasset N. CRMP5 Controls Glioblastoma Cell Proliferation and Survival through Notch-Dependent Signaling. *Cancer Res*. 2015; 75(17):3519–3528. DOI: 10.1158/0008-5472.CAN-14-0631 [PubMed: 26122847]
 24. Wilson SM, Xiong W, Wang Y, Ping X, Head JD, Brittain JM, Gagare PD, Ramachandran PV, Jin X, Khanna R. Prevention of posttraumatic axon sprouting by blocking collapsin response mediator protein 2-mediated neurite outgrowth and tubulin polymerization. *Neuroscience*. 2012; 210:451–466. DOI: 10.1016/j.neuroscience.2012.02.038 [PubMed: 22433297]
 25. Moutal A, Eyde N, Telemi E, Park KD, Xie JY, Dodick DW, Porreca F, Khanna R. Efficacy of (S)-Lacosamide in preclinical models of cephalic pain. *Pain Rep*. 2016; 1(1)doi: 10.1097/PR9.0000000000000565
 26. Moutal A, Chew LA, Yang X, Wang Y, Yeon SK, Telemi E, Meroueh S, Park KD, Shrinivasan R, Gilbraith KB, Qu C, Xie JY, Patwardhan A, Vanderah TW, Khanna M, Porreca F, Khanna R. (S)-lacosamide inhibition of CRMP2 phosphorylation reduces postoperative and neuropathic pain behaviors through distinct classes of sensory neurons identified by constellation pharmacology. *Pain*. 2016; 157(7):1448–1463. DOI: 10.1097/j.pain.0000000000000555 [PubMed: 26967696]
 27. Moutal A, Francois-Moutal L, Perez-Miller S, Cottier K, Chew LA, Yeon SK, Dai J, Park KD, Khanna M, Khanna R. (S)-Lacosamide Binding to Collapsin Response Mediator Protein 2 (CRMP2) Regulates CaV2.2 Activity by Subverting Its Phosphorylation by Cdk5. *Molecular neurobiology*. 2016; 53(3):1959–1976. DOI: 10.1007/s12035-015-9141-2 [PubMed: 25846820]
 28. Bocchini V, Casalone R, Collini P, Rebel G, Lo Curto F. Changes in glial fibrillary acidic protein and karyotype during culturing of two cell lines established from human glioblastoma multiforme. *Cell Tissue Res*. 1991; 265(1):73–81. [PubMed: 1655272]
 29. Clark AJ, Safae M, Oh T, Ivan ME, Parimi V, Hashizume R, Ozawa T, James CD, Bloch O, Parsa AT. Stable luciferase expression does not alter immunologic or in vivo growth properties of GL261 murine glioma cells. *J Transl Med*. 2014; 12:345.doi: 10.1186/s12967-014-0345-4 [PubMed: 25464980]
 30. Brittain JM, Piekarz AD, Wang Y, Kondo T, Cummins TR, Khanna R. An atypical role for collapsin response mediator protein 2 (CRMP-2) in neurotransmitter release via interaction with presynaptic voltage-gated calcium channels. *The Journal of biological chemistry*. 2009; 284(45): 31375–31390. DOI: 10.1074/jbc.M109.009951 [PubMed: 19755421]
 31. Dustrude ET, Moutal A, Yang X, Wang Y, Khanna M, Khanna R. Hierarchical CRMP2 posttranslational modifications control NaV1.7 function. *Proceedings of the National Academy of*

- Sciences of the United States of America. 2016; 113(52):E8443–E8452. DOI: 10.1073/pnas.1610531113 [PubMed: 27940916]
32. Choi D, Stables JP, Kohn H. Synthesis and anticonvulsant activities of N-Benzyl-2-acetamidopropionamide derivatives. *J Med Chem.* 1996; 39(9):1907–1916. [PubMed: 8627614]
 33. Francois-Moutal L, Wang Y, Moutal A, Cottier KE, Melemedjian OK, Yang X, Wang Y, Ju W, Largent-Milnes TM, Khanna M, Vanderah TW, Khanna R. A membrane-delimited N-myristoylated CRMP2 peptide aptamer inhibits CaV2.2 trafficking and reverses inflammatory and postoperative pain behaviors. *Pain.* 2015; 156(7):1247–1264. DOI: 10.1097/j.pain.000000000000147 [PubMed: 25782368]
 34. Dustrude ET, Wilson SM, Ju W, Xiao Y, Khanna R. CRMP2 protein SUMOylation modulates NaV1.7 channel trafficking. *The Journal of biological chemistry.* 2013; 288(34):24316–24331. DOI: 10.1074/jbc.M113.474924 [PubMed: 23836888]
 35. Cook RL, Householder KT, Chung EP, Prakapenka AV, DiPerna DM, Sirianni RW. A critical evaluation of drug delivery from ligand modified nanoparticles: Confounding small molecule distribution and efficacy in the central nervous system. *J Control Release.* 2015; 220(Pt A):89–97. DOI: 10.1016/j.jconrel.2015.10.013 [PubMed: 26471392]
 36. Abdelwahab MG, Sankar T, Preul MC, Scheck AC. Intracranial implantation with subsequent 3D in vivo bioluminescent imaging of murine gliomas. *J Vis Exp.* 2011; (57):e3403.doi: 10.3791/3403 [PubMed: 22158303]
 37. Householder KT, DiPerna DM, Chung EP, Wohlleb GM, Dhruv HD, Berens ME, Sirianni RW. Intravenous delivery of camptothecin-loaded PLGA nanoparticles for the treatment of intracranial glioma. *Int J Pharm.* 2015; 479(2):374–380. DOI: 10.1016/j.ijpharm.2015.01.002 [PubMed: 25562639]
 38. Cole AR, Knebel A, Morrice NA, Robertson LA, Irving AJ, Connolly CN, Sutherland C. GSK-3 phosphorylation of the Alzheimer epitope within collapsin response mediator proteins regulates axon elongation in primary neurons. *The Journal of biological chemistry.* 2004; 279(48):50176–50180. DOI: 10.1074/jbc.C400412200 [PubMed: 15466863]
 39. Koo TS, Kim SJ, Ha DJ, Baek M, Moon H. Pharmacokinetics, brain distribution, and plasma protein binding of the antiepileptic drug lacosamide in rats. *Archives of pharmacological research.* 2011; 34(12):2059–2064. DOI: 10.1007/s12272-011-1208-7 [PubMed: 22210031]
 40. Elizabeth, W., Newcomb, DZ. The Murine GL261 Glioma Experimental Model to Assess Novel Brain Tumor Treatments. In: Erwin, G., Van Meir, P., editors. *Models, Markers, Prognostic Factors, Targets, and Therapeutic Approaches.* Humana Press; 2009. p. 227–241.
 41. Toledo CM, Ding Y, Hoellerbauer P, Davis RJ, Basom R, Girard EJ, Lee E, Corrin P, Hart T, Bolouri H, Davison J, Zhang Q, Hardcastle J, Aronow BJ, Plaisier CL, Baliga NS, Moffat J, Lin Q, Li XN, Nam DH, Lee J, Pollard SM, Zhu J, Delrow JJ, Clurman BE, Olson JM, Paddison PJ. Genome-wide CRISPR-Cas9 Screens Reveal Loss of Redundancy between PKMYT1 and WEE1 in Glioblastoma Stem-like Cells. *Cell Rep.* 2015; 13(11):2425–2439. DOI: 10.1016/j.celrep.2015.11.021 [PubMed: 26673326]
 42. Cole AR, Causeret F, Yadirgi G, Hastie CJ, McLauchlan H, McManus EJ, Hernandez F, Eickholt BJ, Nikolic M, Sutherland C. Distinct priming kinases contribute to differential regulation of collapsin response mediator proteins by glycogen synthase kinase-3 in vivo. *The Journal of biological chemistry.* 2006; 281(24):16591–16598. DOI: 10.1074/jbc.M513344200 [PubMed: 16611631]
 43. Cole AR, Soutar MP, Rembutsu M, van Aalten L, Hastie CJ, McLauchlan H, Peggie M, Balastik M, Lu KP, Sutherland C. Relative resistance of Cdk5-phosphorylated CRMP2 to dephosphorylation. *The Journal of biological chemistry.* 2008; 283(26):18227–18237. DOI: 10.1074/jbc.M801645200 [PubMed: 18460467]
 44. Balastik M, Zhou XZ, Alberich-Jorda M, Weissova R, Ziak J, Pazyra-Murphy MF, Cosker KE, Machonova O, Kozmikova I, Chen CH, Pastorino L, Asara JM, Cole A, Sutherland C, Segal RA, Lu KP. Prolyl Isomerase Pin1 Regulates Axon Guidance by Stabilizing CRMP2A Selectively in Distal Axons. *Cell Rep.* 2015; 13(4):812–828. DOI: 10.1016/j.celrep.2015.09.026 [PubMed: 26489457]

45. Kamiya Y, Saeki K, Takiguchi M, Funakoshi K. CDK5, CRMP2 and NR2B in spinal dorsal horn and dorsal root ganglion have different role in pain signaling between neuropathic pain model and inflammatory pain model. *European Journal of Anaesthesiology*. 2013; 30:214–214.
46. Korur S, Huber RM, Sivasankaran B, Petrich M, Morin P Jr, Hemmings BA, Merlo A, Lino MM. GSK3beta regulates differentiation and growth arrest in glioblastoma. *PLoS one*. 2009; 4(10):e7443.doi: 10.1371/journal.pone.0007443 [PubMed: 19823589]
47. Domoto T, Pyko IV, Furuta T, Miyashita K, Uehara M, Shimasaki T, Nakada M, Minamoto T. Glycogen synthase kinase-3beta is a pivotal mediator of cancer invasion and resistance to therapy. *Cancer Sci*. 2016; 107(10):1363–1372. DOI: 10.1111/cas.13028 [PubMed: 27486911]
48. Pyko IV, Nakada M, Sabit H, Teng L, Furuyama N, Hayashi Y, Kawakami K, Minamoto T, Fedulau AS, Hamada J. Glycogen synthase kinase 3beta inhibition sensitizes human glioblastoma cells to temozolomide by affecting O6-methylguanine DNA methyltransferase promoter methylation via c-Myc signaling. *Carcinogenesis*. 2013; 34(10):2206–2217. DOI: 10.1093/carcin/bgt182 [PubMed: 23715499]
49. Schiel JA, Park K, Morphew MK, Reid E, Hoenger A, Prekeris R. Endocytic membrane fusion and buckling-induced microtubule severing mediate cell abscission. *J Cell Sci*. 2011; 124(Pt 9):1411–1424. DOI: 10.1242/jcs.081448 [PubMed: 21486954]
50. Fremont S, Romet-Lemonne G, Houdusse A, Echard A. Emerging roles of MICAL family proteins - from actin oxidation to membrane trafficking during cytokinesis. *J Cell Sci*. 2017; doi: 10.1242/jcs.202028
51. Brittain JM, Wang Y, Eruvwetere O, Khanna R. Cdk5-mediated phosphorylation of CRMP-2 enhances its interaction with CaV2.2. *FEBS letters*. 2012; 586(21):3813–3818. DOI: 10.1016/j.febslet.2012.09.022 [PubMed: 23022559]
52. Uchida Y, Ohshima T, Sasaki Y, Suzuki H, Yanai S, Yamashita N, Nakamura F, Takei K, Ihara Y, Mikoshiba K, Kolattukudy P, Honnorat J, Goshima Y. Semaphorin3A signalling is mediated via sequential Cdk5 and GSK3beta phosphorylation of CRMP2: implication of common phosphorylating mechanism underlying axon guidance and Alzheimer's disease. *Genes to cells : devoted to molecular & cellular mechanisms*. 2005; 10(2):165–179. DOI: 10.1111/j.1365-2443.2005.00827.x [PubMed: 15676027]
53. Schmidt EF, Shim SO, Strittmatter SM. Release of MICAL autoinhibition by semaphorin-plexin signaling promotes interaction with collapsin response mediator protein. *The Journal of neuroscience : the official journal of the Society for Neuroscience*. 2008; 28(9):2287–2297. DOI: 10.1523/JNEUROSCI.5646-07.2008 [PubMed: 18305261]
54. Bagci T, Wu JK, Pfannl R, Ilag LL, Jay DG. Autocrine semaphorin 3A signaling promotes glioblastoma dispersal. *Oncogene*. 2009; 28(40):3537–3550. DOI: 10.1038/onc.2009.204 [PubMed: 19684614]
55. Santolini E, Puri C, Salcini AE, Gagliani MC, Pelicci PG, Tacchetti C, Di Fiore PP. Numb is an endocytic protein. *J Cell Biol*. 2000; 151(6):1345–1352. [PubMed: 11121447]
56. See WL, Tan IL, Mukherjee J, Nicolaides T, Pieper RO. Sensitivity of glioblastomas to clinically available MEK inhibitors is defined by neurofibromin 1 deficiency. *Cancer Res*. 2012; 72(13):3350–3359. DOI: 10.1158/0008-5472.CAN-12-0334 [PubMed: 22573716]
57. Han S, Meng L, Jiang Y, Cheng W, Tie X, Xia J, Wu A. Lithium enhances the antitumour effect of temozolomide against TP53 wild-type glioblastoma cells via NFAT1/FasL signalling. *Br J Cancer*. 2017; doi: 10.1038/bjc.2017.89
58. Adamo A, Fiore D, De Martino F, Roscigno G, Affinito A, Donnarumma E, Puoti I, Ricci-Vitiani L, Pallini R, Quintavalle C, Condorelli G. RYK promotes the stemness of glioblastoma cells via the WNT/ beta-catenin pathway. *Oncotarget*. 2017; doi: 10.18632/oncotarget.14564
59. Wu A, Oh S, Wiesner SM, Ericson K, Chen L, Hall WA, Champoux PE, Low WC, Ohlfest JR. Persistence of CD133+ cells in human and mouse glioma cell lines: detailed characterization of GL261 glioma cells with cancer stem cell-like properties. *Stem Cells Dev*. 2008; 17(1):173–184. DOI: 10.1089/scd.2007.0133 [PubMed: 18271701]
60. Moutal A, Chew LA, Yang X, Wang Y, Yeon SK, Telemi E, Meroueh S, Park KD, Shrinivasan R, Gilbraith KB, Qu C, Xie JY, Patwardhan A, Vanderah TW, Khanna M, Porreca F, Khanna R. (S)-Lacosamide inhibition of CRMP2 phosphorylation reduces postoperative and neuropathic pain

behaviors through distinct classes of sensory neurons identified by constellation pharmacology.
Pain. 2016; doi: 10.1097/j.pain.0000000000000555

Author Manuscript

Author Manuscript

Author Manuscript

Author Manuscript

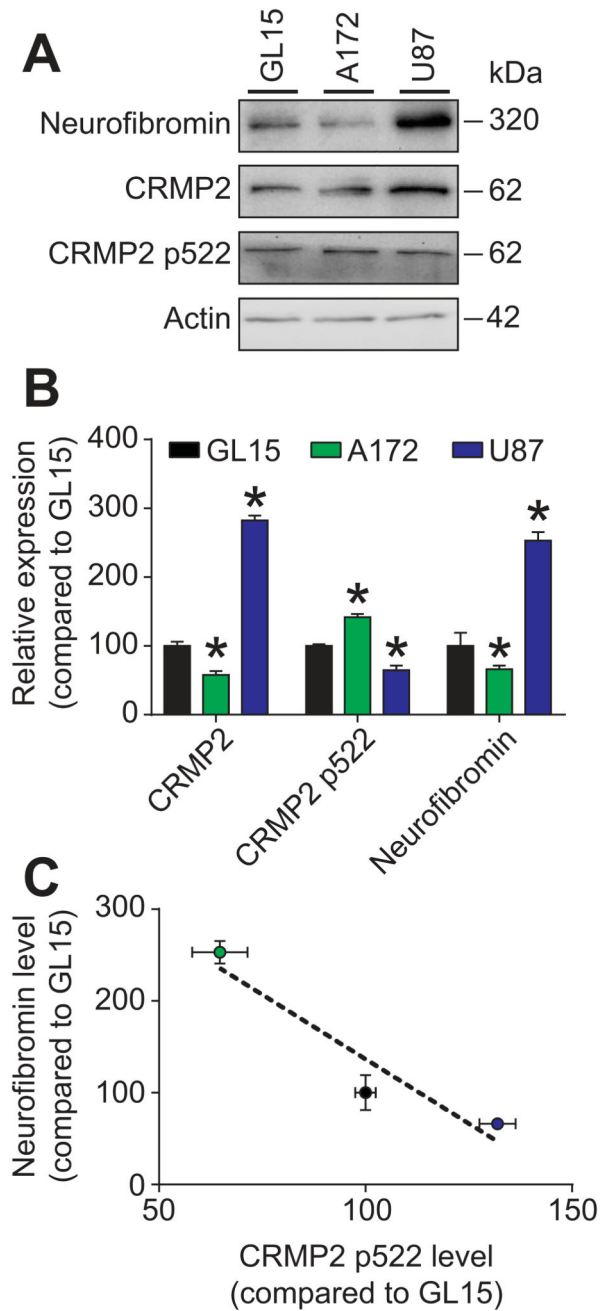


Figure 1. Neurofibromin expression correlates inversely with CRMP2 phosphorylation level in GBM cell lines

(A) Representative immunoblots from lysates of human GL15, A172 and U87 cells probed for neurofibromin, total CRMP2 and Cdk5-phosphorylated CRMP2 (at serine 522; p522). Actin is used as a loading control. (B) Bar graph showing the relative expression level of neurofibromin, total CRMP2 and CRMP2 p522 in GL15, A172 and U87 cells. Neurofibromin and CRMP2 were more expressed in U87 and CRMP2 phosphorylation was higher in A172 cells. * $p < 0.05$ vs. GL15, Kruskal-Wallis test, $n = 3$ independent experiments. (C) Graph showing the correlation between neurofibromin and CRMP2 phosphorylation

levels in GL15, A172 and U87 cell lines. The dotted line shows an inverse correlation between neurofibromin and CRMP2 phosphorylation levels.

Author Manuscript

Author Manuscript

Author Manuscript

Author Manuscript

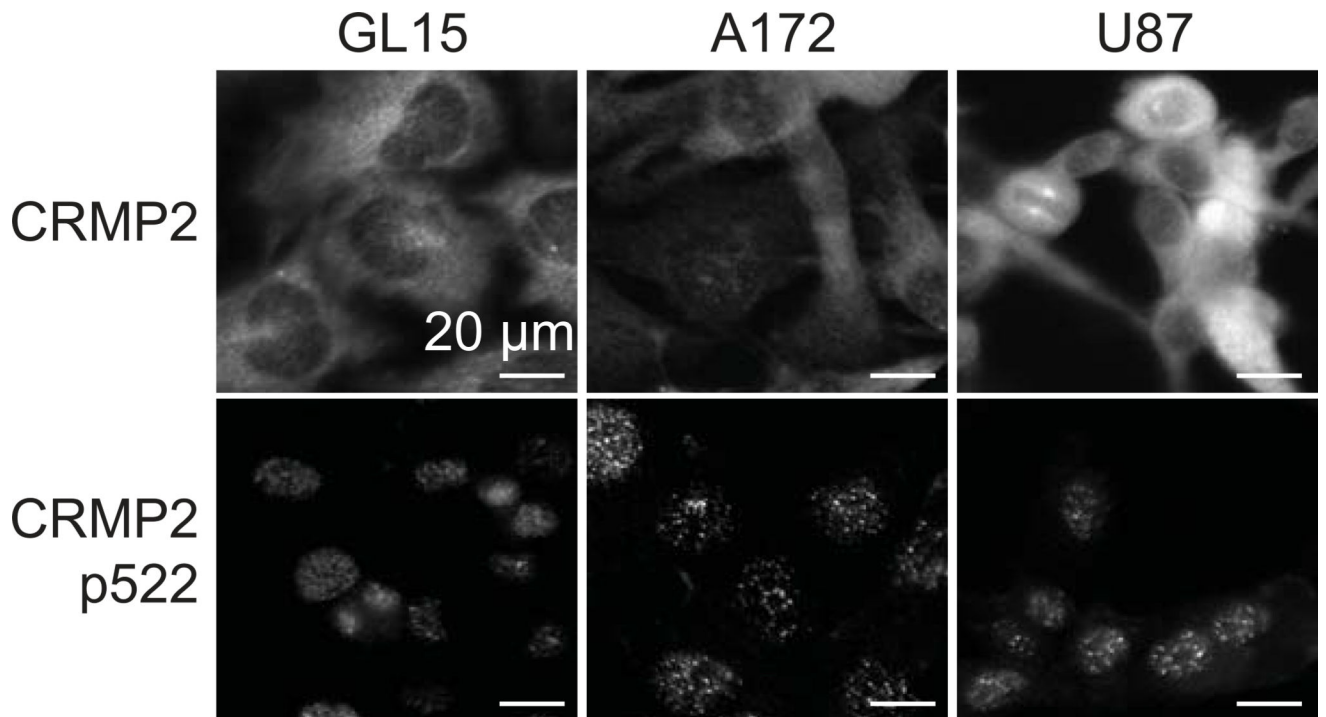


Figure 2. Phosphorylated CRMP2 is localized in the nucleus of glioblastoma cells
Representative immunofluorescence of GL15, A172 or U87 cells stained for either CRMP2 (top panels) or CRMP2 p522 (bottom panels). The scale is 20 μm for all panels. Micrographs show cytosolic and nuclear localization of total CRMP2 while Cdk5-phosphorylated CRMP2 (at serine 522; p522) is found exclusively in the nucleus.

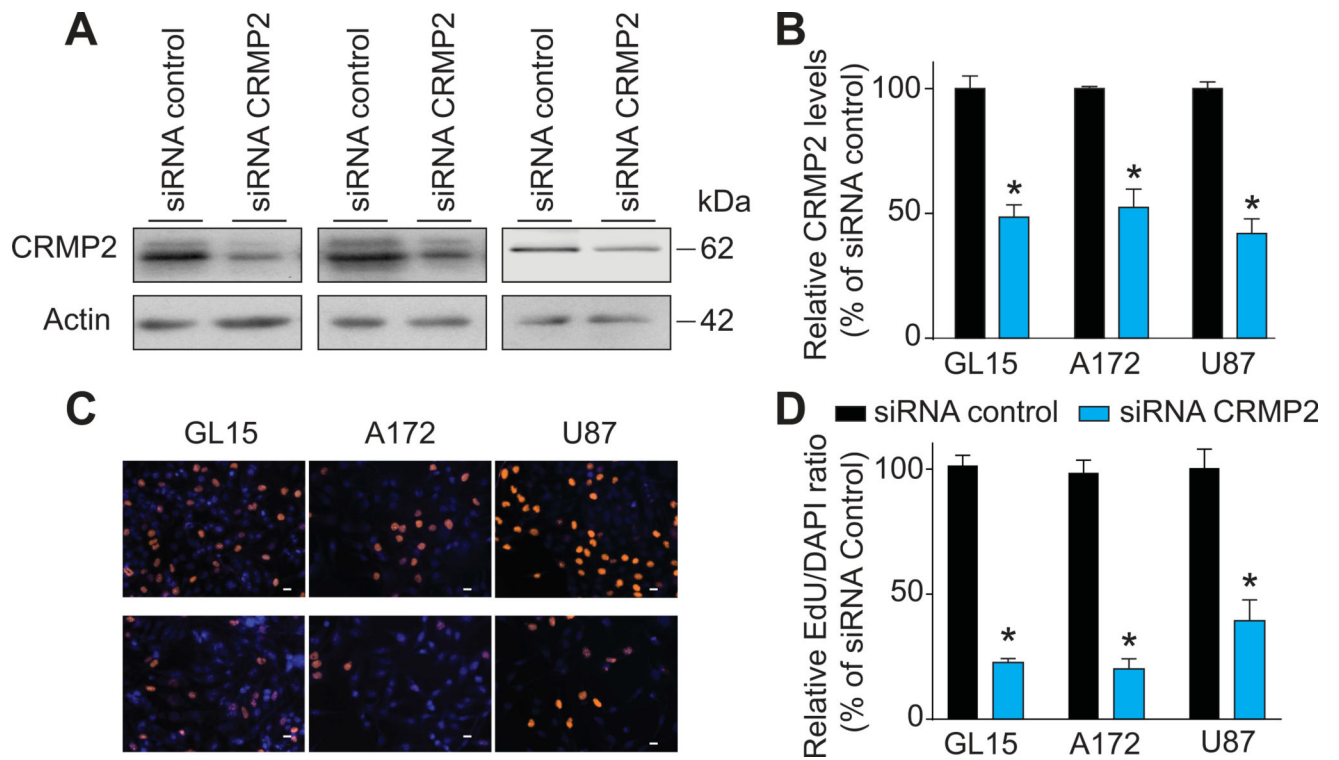


Figure 3. Glioblastoma proliferation requires CRMP2 expression

(A) Representative immunoblots of GL15, A172 or U87 cell lysates after transfection with either a control siRNA or CRMP2 siRNA. The blots were probed with CRMP2 or actin as a loading control. (B) Bar graph showing the relative CRMP2 expression levels in GL15, A172 or U87 cells after transfection with CRMP2 siRNA. CRMP2 expression was reduced by the CRMP2 siRNA transfection compared to control siRNA. * $p < 0.05$ vs. control siRNA, Mann Whitney test, $n = 3$ independent experiments. (C) Representative micrographs of GL15, A172 or U87 cells stained for EdU incorporation after transfection with either a control or CRMP2 siRNA. The scale bar is 10 μm . DAPI was used to stain the nucleus of all cells. (D) Bar graph showing the proliferation ratio (EdU/DAPI) of GL15, A172 or U87 cells after transfection with CRMP2 siRNA, normalized to control siRNA level. Knockdown of CRMP2 decreased the proliferation of GL15, A172 and U87 cells. * $p < 0.05$ vs. siRNA control, Mann Whitney test, $n = 10\text{--}12$ coverslips per group from 3 independent experiments.

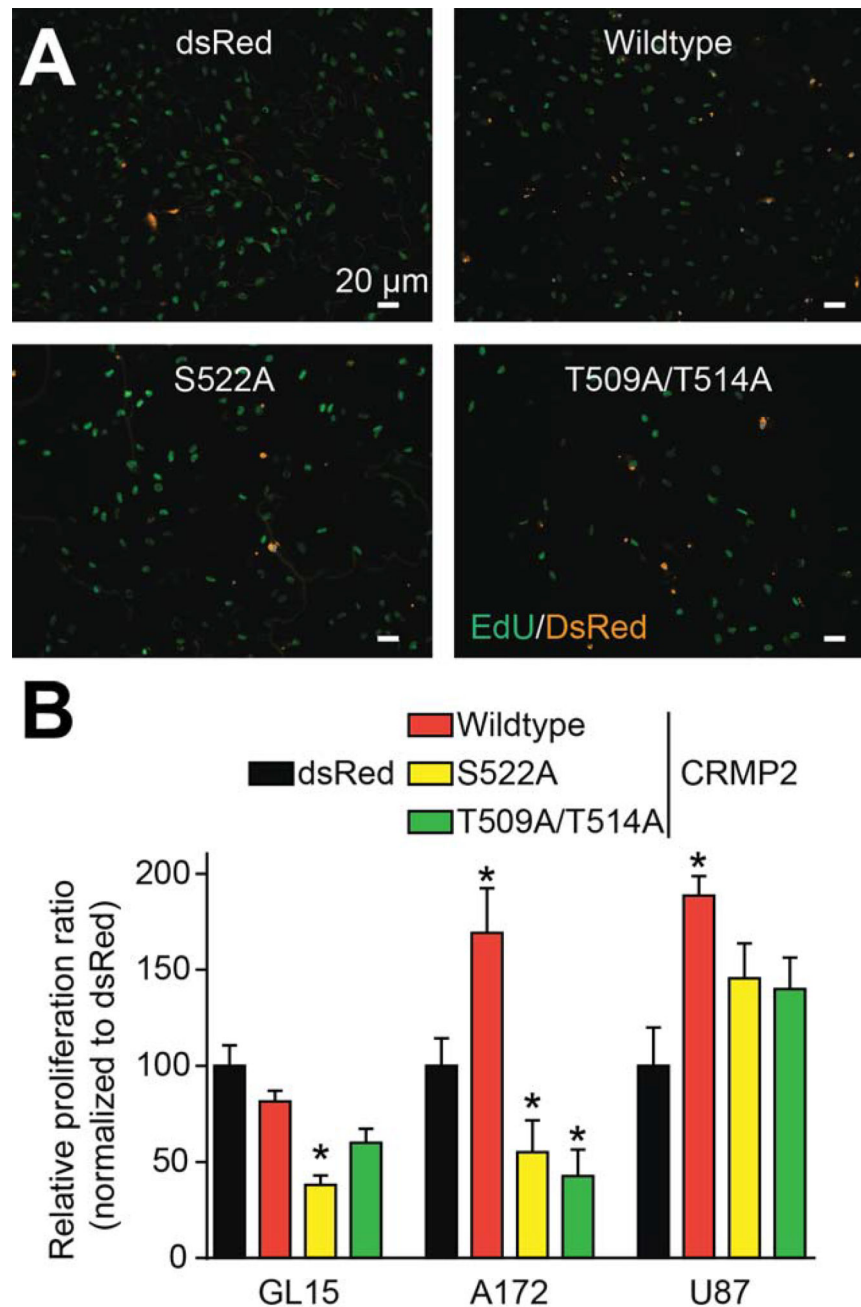


Figure 4. Glioblastoma proliferation is controlled by CRMP2 expression and phosphorylation

(A) Representative micrographs of GL15 cells transfected by either empty, wildtype-CRMP2, CRMP2 S522A or CRMP2 T509A/T514A expressing pdsRed-N2 plasmids. Transfected cells were identified by dsRed fluorescence; proliferating cells were stained for Edu incorporation; and cell nuclei were stained with DAPI (not shown here). Scale bar is 20 μ m. (B) Bar graph showing the proliferation ratio (EdU/DAPI) of GL15, A172 or U87 cells after transfection with the indicated plasmids, normalized to empty plasmid level. CRMP2 wildtype expression increased proliferation for A172 and U87 cells. CRMP2 S522A expression decreased the proliferation of GL15 and A172 cells. CRMP2 T509A/T514A

expression decreased the proliferation of A172 cells. * $p < 0.05$ vs. dsRed, Kruskal-wallis test, $n = 10-12$ coverslips per group from 3 independent experiments.

Author Manuscript

Author Manuscript

Author Manuscript

Author Manuscript

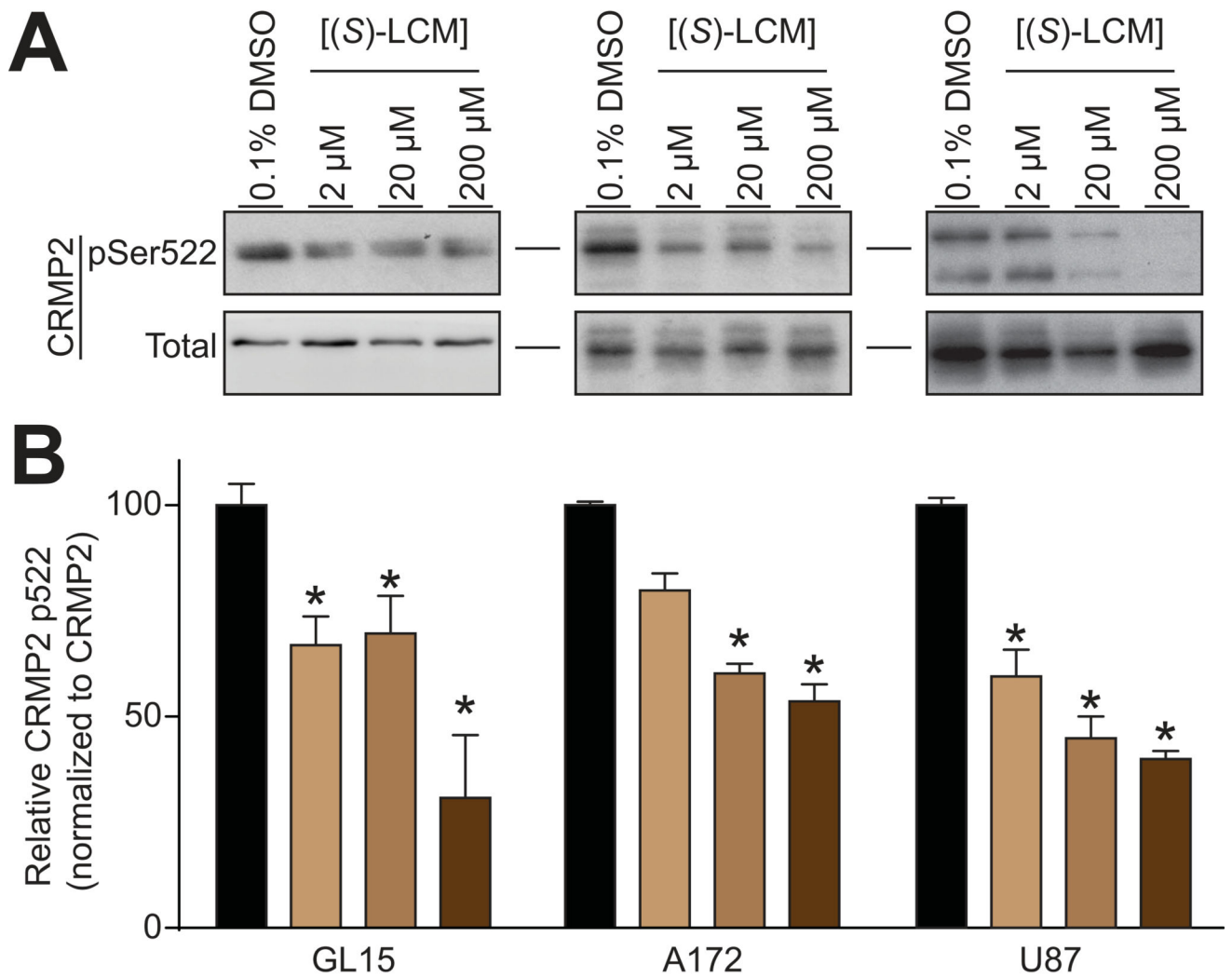


Figure 5. (S)-lacosamide inhibits CRMP2 phosphorylation in glioblastoma cell lines

(A) Representative immunoblots of GL15, A172 and U87 lysates after treatment overnight with the indicated (S)-lacosamide concentrations or 0.1% DMSO (vehicle). Lysates were probed with anti-CRMP2 (total) and anti-CRMP2 pSer522 antibodies. (B) Bar graph showing the relative CRMP2 phosphorylation level, normalized to CRMP2 expression level and to 0.1% DMSO for each cell line. CRMP2 phosphorylation was reduced by (S)-lacosamide treatment in all cell lines. * $p < 0.05$ vs. DMSO, Kruskal-wallis test, $n = 3$ per group independent experiments.

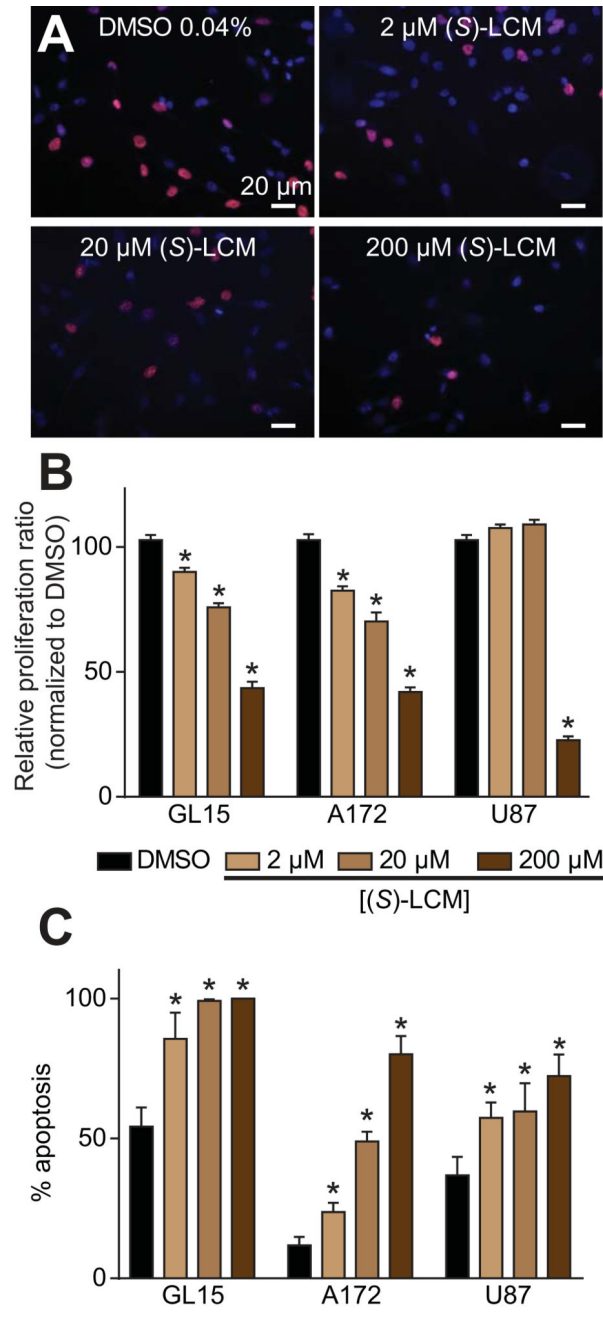


Figure 6. (S)-lacosamide inhibits proliferation and induces apoptosis in glioblastoma cell lines (A) Representative micrographs of GL15 cells treated overnight with the indicated (S)-lacosamide concentration or 0.04% DMSO (vehicle). Proliferating cells were stained for Edu incorporation (red), cell nuclei were stained with DAPI (blue). Scale bar is 20 μ m. (B) Bar graph showing the relative proliferation ratio (EdU/DAPI), normalized to 0.1% DMSO for each cell line. GBM cell proliferation was reduced by (S)-lacosamide treatment in all cell lines. * p <0.05 vs. DMSO, Kruskal-wallis test, n =10–12 coverslips per group from 3 independent experiments. (C) Bar graph showing the relative apoptosis rate (%) normalized to 0.04% DMSO for each cell line. GBM cell apoptosis rate was increased by (S)-

lacosamide treatment in all cell lines. * $p < 0.05$ vs. DMSO, Kruskal-wallis test, $n = 10-12$ coverslips per group from 3 independent experiments.

Author Manuscript

Author Manuscript

Author Manuscript

Author Manuscript

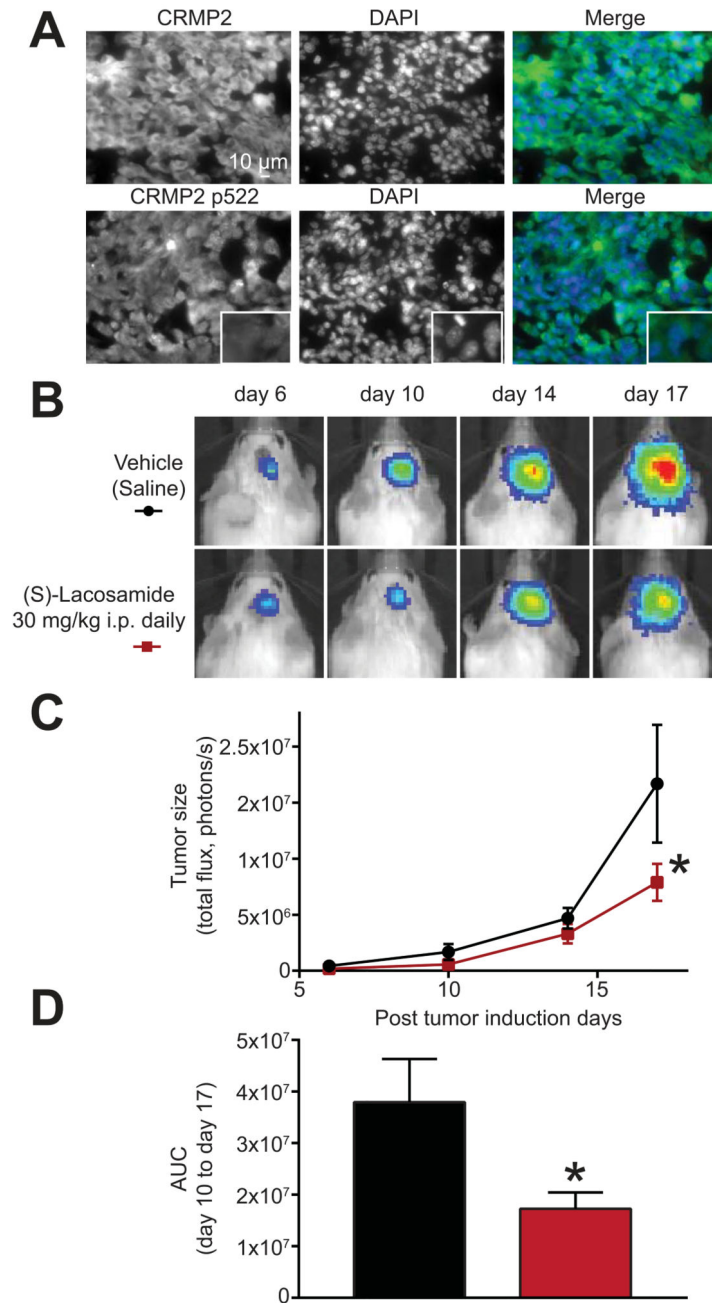


Figure 7. (S)-lacosamide decreases glioblastoma growth in vivo

(A) Micrographs of a 10- μ m section of a brain slice injected with GL261 cells immunostained with CRMP2 or p522-CRMP2. A merged image (CRMP2/p522-CRMP2 and DAPI (nuclear stain)) shows nuclear localization of phosphorylated CRMP2. Higher magnification (inset) shows the staining pattern of phosphorylated CRMP2 within the nucleus. (B) Representative pictures showing the bioluminescence intensity of the intracranial GBM tumor before (day 6) and during the course of the treatment with (S)-lacosamide (30 mg/kg, i.p. daily) or vehicle (saline). (C) Graph showing the tumor size, measured by number of photons per second, before (day 6) and during the course of the

treatment by either (S)-lacosamide (30 mg/kg i.p. daily) or Saline (vehicle). Tumor size was significantly smaller after 10 days of treatment with (S)-lacosamide compared to saline (n=5 per group, Sidak's correction for multiple comparisons applied to a two-way repeat measure ANOVA). (D) Bar graph showing the area under the curve (AUC) between day 10 and day 17. (S)-lacosamide treatment significantly decreased the AUC compared to saline treatment (n=5 per group, two-tailed Student's t test). Statistical significance denoted by *p<0.05

Author Manuscript

Author Manuscript

Author Manuscript

Author Manuscript